THE JOURNAL OF BIOLOGICAL CHEMISTRY VOL. 282, NO. 5, pp. 3146–3156, February 2, 2007

Differential Helical Orientations among Related G Protein-coupled Receptors Provide a Novel Mechanism for Selectivity

*STUDIES WITH SALVINORIN A AND THE κ-OPIOID RECEPTOR**

Received for publication, September 29, 2006, and in revised form, November 15, 2006 Published, JBC Papers in Press, November 22, 2006, DOI 10.1074/jbc.M609264200

Timothy A. Vortherms[‡§], Philip D. Mosier[¶], Richard B. Westkaemper[¶], and Bryan L. Roth[‡§‖1]**

*From the Departments of [‡]Biochemistry, [‖]Psychiatry, and **Neurosciences, Case Western Reserve University School of Medicine, Cleveland, Ohio 44106, the [§]Department of Pharmacology, University of North Carolina School of Medicine, Chapel Hill, North Carolina 27599, and the [¶]Department of Medicinal Chemistry, Virginia Commonwealth University, Richmond, Virginia 23298*

Salvinorin A, the active component of the hallucinogenic sage *Salvia divinorum*, is an apparently selective and highly potent κ-opioid receptor (KOR) agonist. Salvinorin A is unique among ligands for peptidergic G protein-coupled receptors in being nonnitrogenous and lipid-like in character. To examine the molecular basis for the subtype-selective binding of salvinorin A, we utilized an integrated approach using chimeric opioid receptors, site-directed mutagenesis, the substituted cysteine accessibility method, and molecular modeling and dynamics studies. We discovered that helix 2 is required for salvinorin A binding to KOR and that two residues (Val-108(2.53) and Val-118(2.63)) confer subtype selectivity. Intriguingly, molecular modeling studies predicted that these loci exhibit an indirect effect on salvinorin A binding, presumably through rotation of helix 2. Significantly, and in agreement with our *in silico* predictions, substituted cysteine accessibility method analysis of helix 2 comparing KOR and the δ-opioid receptor, which has negligible affinity for salvinorin A, revealed that residues known to be important for salvinorin A binding exhibit a differential pattern of water accessibility. These findings imply that differences in the helical orientation of helix 2 are critical for the selectivity of salvinorin A binding to KOR and provide a structurally novel basis for ligand selectivity.

Salvia divinorum, a member of the sage family, is a hallucinogenic plant that has been used for traditional spiritual purposes by Mazatec shamans of Oaxaca, Mexico (1, 2). More recently, *S. divinorum* leaves and extracts have been used as legal hallucinogens in the United States. The active compound of *S. divinorum* is the neoclerodane diterpene salvinorin A, which is comparable in potency with the synthetic hallucinogen lysergic acid diethylamide (3, 4). Following extensive screening of the receptorome, we identified the κ-opioid receptor (KOR)[2] as the molecular target of salvinorin A (5). Salvinorin A has negligible affinity for all other tested G protein-coupled receptors (GPCRs), including the μ- and δ-opioid receptors (MOR and DOR), as well as serotonin 5-HT_{2A} receptors (5, 6), which represent the molecular target for classical hallucinogens (7).

Salvinorin A is both pharmacologically and chemically unique in that it represents the first nonnitrogenous, naturally occurring KOR-selective agonist and the only known nonalkaloidal hallucinogen. Given that salvinorin A lacks the basic amino group present in all other KOR-selective ligands (for a review, see Ref. 8), ionic interactions are unlikely to stabilize salvinorin A in the binding pocket of KOR (9, 10). This has led to the hypothesis that salvinorin A binding at KOR may involve novel ligand-receptor interactions that utilize distinct residues within a conserved ligand binding pocket (10).

Site-directed mutagenesis and molecular modeling studies have been widely used to gain insight into the mechanisms of receptor-ligand binding interactions (11–14). In fact, recent mutagenesis and molecular modeling studies have demonstrated that salvinorin A is stabilized in the KOR binding pocket via hydrophobic and hydrogen bonding interactions with Gln-115(2.60) and Tyr-119(2.64) in TM2 and Tyr-313(7.36) and Tyr-320(7.43) in TM7 (9, 10). As expected, mutation of the highly conserved Asp-138(3.32) in TM3, which is thought to form an ionic interaction with the positively charged amino group of opioid ligands (8), did not markedly alter salvinorin A binding (9). Interestingly, most of the hydrophobic and hydrogen binding loci are conserved among KOR, DOR, and MOR, suggesting that there is considerable overlap in the salvinorin A binding pocket across all opioid receptor subtypes. This finding that salvinorin A utilizes conserved residues for binding fails, however, to explain the molecular basis for the exquisite subtype selectivity of salvinorin A. Based on these observations, it is tempting to speculate that receptor subtype differences in the orientation of transmembrane helices may preclude salvinorin A-receptor binding interactions in DOR and MOR.

* This work was supported by National Institutes of Health Grants RO1DA017204 (to B. L. R.), 5T32HL007653-17 (to T. A. V.), and 1F32DA022188-01 (to T. A. V.). The costs of publication of this article were defrayed in part by the payment of page charges. This article must therefore be hereby marked "*advertisement*" in accordance with 18 U.S.C. Section 1734 solely to indicate this fact.

[1] To whom correspondence should be addressed: Dept. of Pharmacology, University of North Carolina, CB# 7365, 8032 Burnett-Womack Bldg., Chapel Hill, NC 27599. Tel.: 919-966-7535; Fax: 919-843-5788; E-mail: bryan_roth@med.unc.edu.

[2] The abbreviations used are: KOR, DOR, and MOR, κ-, δ-, and μ-opioid receptor, respectively; SCAM, substituted cysteine accessibility method; MTSEA, (2-aminoethyl)methane thiosulfonate hydrobromide; GPCR, G protein-coupled receptor; TM, transmembrane; E1 and E2 loop, first and second extracellular loop, respectively; MD, molecular dynamics; HEK, human embryonic kidney; SBB, standard binding buffer.

In the absence of direct crystallographic data, the substituted cysteine accessibility method (SCAM) has been used to provide structural information on residues that line the ligand-binding pocket of G protein-coupled receptors, including the D_2 dopamine receptor (15–18) as well as the opioid receptor family (19–21). In the present study, we utilized a combination of approaches to elucidate the molecular determinants essential for the subtype-selective binding of salvinorin A to KOR. To this end, we constructed an extensive series of chimeric opioid receptors wherein transmembrane segments and loop regions of the "salvinorin A-sensitive" KOR and the "salvinorin A-insensitive" DOR and MOR were exchanged in order to identify receptor domains involved in stabilizing salvinorin A binding interactions. The receptor subtype selectivity of salvinorin A was further examined using site-directed mutants of KOR and molecular modeling studies of the salvinorin A-KOR binding complex. We now report that TM2 and, to a lesser extent, the E2 loop of KOR are essential for the selective binding of salvinorin A to KOR. We also report that Val-108(2.53) and Val-118(2.63) in TM2 are critical in conferring the subtype-selective binding of salvinorin A to KOR. Most importantly, SCAM analysis of TM2 in KOR and DOR revealed marked differences in the water accessibility of residues known to be involved in salvinorin A binding. These observations are consistent with molecular modeling studies that predict a helical rotation of TM2 is critical for the subtype selectivity of salvinorin A.

EXPERIMENTAL PROCEDURES

Materials—[^{3}H]Diprenorphine was obtained from Perkin-Elmer Life Sciences (53 Ci/mmol). The standard reagents, unless otherwise stated, were purchased from Sigma. Salvinorin A was obtained from two sources, including the *Salvia divinorum* Research and Information Center (Malibu, CA) and Dr. Thomas Prisinzano (University of Iowa). MTSEA was purchased from Anatrace, Inc. (Maumee, OH).

Cell Culture and Transfection—Human embryonic kidney (HEK) 293T cells were maintained in Dulbecco's modified Eagle's medium supplemented with 10% fetal bovine serum and 1 mM sodium pyruvate (Invitrogen) and were grown in a humidified incubator in the presence of 5% CO_2 at 37 °C. Transient transfection (48 h) of wild-type, chimeric, and mutant receptor cDNAs was performed in 10-cm tissue culture plates using Lipofectamine 2000 (Invitrogen) or EasyTransgater DNA/RNA transfection reagent (America Pharma Source) following the manufacturer's protocol.

Chimeric Receptor Constructs and Site-directed Mutagenesis—The human KOR and MOR cDNAs cloned into the mammalian expression vector pcDNA3.1$^+$ (Invitrogen) were obtained from the UMR cDNA Resource Center (GenBank^{TM} accession number AF498922 and AY521028, respectively). The mouse DOR cDNA (GenBank^{TM} accession number L07271) was a generous gift from Dr. Mark von Zastrow (University of California, San Francisco). Site-directed mutagenesis was performed using the QuikChange® mutagenesis kit (Stratagene) according to the manufacturer's protocol. Amino acids were labeled as described previously (14, 19). The DOR (L110(2.65)C-A98(2.53)C) cysteine mutants were constructed using the wild-type DOR template, whereas the KOR (L120(2.65)C-V108(2.53)C) cysteine mutants were constructed using the MTSEA-insensitive C315(7.38)S KOR template. These cysteine mutants were subsequently subcloned into the pBabePuro retroviral vector (22) for transient expression in HEK 293T cells. The incorporation of receptor mutations was verified using PCR-based, automated DNA sequencing (Cleveland Genomics (Cleveland, OH) and Biotic Solutions (New York, NY)).

The generation of cross-subtype KOR-DOR and KOR-MOR chimeras was completed using an overlapping PCR-based method. For this cloning strategy, the DNA primers (Invitrogen) were designed with ~20 nucleotides complementary to the KOR cDNA at the junction sites listed below and an additional ~20 nucleotides of overhang that were complementary to the DOR or MOR cDNAs at the appropriate splicing site. The initial receptor fragments were amplified using PCR under the following conditions: initial denaturation at 95 °C (45 s) and then 30 cycles of 95 °C (45 s), 50 °C (45 s), and 72 °C (1.5 min), followed by a terminal extension at 72 °C (10 min); 100 ng of plasmid DNA, 0.75 μM each primer, 500 μM deoxyribonucleoside triphosphates (Roche Applied Science), 1 unit of Pfu Turbo DNA polymerase (Stratagene). The resulting PCR fragments were purified from a 1–2% agarose gel using the QIAquick gel extraction kit (Qiagen) and combined for subsequent rounds of PCR. The ~20 nucleotide overhangs allowed the KOR and DOR/MOR fragments to anneal to each other, resulting in the recombination of KOR-DOR and KOR-MOR cDNAs at the engineered splice sites. The annealed DNA fragments served as the template for the second round of PCR, which was completed as described above except that the first five cycles were completed in the absence of primers to allow for extension of the annealed KOR-DOR and KOR-MOR fragments.

The resulting $KOR_{(TM1-4,E2L)}$-$DOR_{(TM5-7)}$ chimera encoded amino acids Met-1 to Met-226 of KOR and Lys-214 to Ala-372 of DOR, and the $DOR_{(TM1-4,E2L)}$-$KOR_{(TM5-7)}$ chimera encoded amino acids Met-1 to Thr-213 of DOR and Lys-227 to Val-380 of KOR. The KOR-$DOR_{(TM1)}$ chimera encoded amino acids Met-1 to Arg-76 of DOR (N-terminus to TM1) and amino acids Tyr-87 to Val-380 of KOR (I1 loop to the C terminus). The KOR-$DOR_{(TM2)}$ chimera encoded amino acids Met-1 to Arg-86 (N-terminus to TM1) and Tyr-119 to Val-380 (E1 loop to the C terminus) of KOR and amino acids Tyr-77 to Lys-108 of DOR (I1 loop to TM2). The KOR-$DOR_{(TM4)}$ chimera encoded amino acids Met-1 to Pro-172 (N terminus to the I2 loop) and Leu-196 to Val-380 (E2 loop to the C terminus) of KOR and amino acids Ala-163 to Val-185 (TM4) of DOR. The KOR-$DOR_{(E2L)}$ chimera encoded amino acids Met-1 to Val-195 (N terminus to TM4) and Lys-227 to Val-380 (TM5 to the C terminus) of KOR and amino acids Met-186 to Thr-213 of DOR (E2 loop). The salvinorin A-rescue chimera DOR-$KOR_{(TM1)}$ encoded amino acids Met-1 to Arg-86 (N terminus to TM1) of KOR and Tyr-77 to Ala-372 (I1 loop to the C terminus) of DOR. The DOR-$KOR_{(TM1,TM2)}$ chimera encoded amino acids Met-1 to Val-118 of KOR (N terminus to TM2) and amino acids Tyr-109 to Ala-372 of DOR (E1 loop to the C terminus). The DOR-$KOR_{(TM2,E2L)}$ chimera encoded amino acids Met-1 to Arg-76 (N-terminus to TM1), Tyr-109 to Val-185 (E1 loop to TM4), and Lys-214 to Ala-372 (TM5 to the C terminus) of DOR and amino acids Tyr-87 to Val-118 (I1 loop to TM2) and Leu-196 to Met-226 (E2 loop) of KOR. The MOR-$KOR_{(TM2,E2L)}$ chimera

encoded amino acids Met-1 to Thr-103 (N-terminus to the I1 loop), Tyr-130 to Phe-206 (E1 loop to TM4), and Lys-235 to Pro-400 (TM5 to the C terminus) of MOR and amino acids Ala-93 to Val-118 (TM2) and Leu-196 to Met-226 (E2 loop) of KOR. The sequence of engineered receptors was verified using PCR-based, automated DNA sequencing (Cleveland Genomics (Cleveland, OH) and Biotic Solutions (New York, NY)).

Radioligand Binding Assays—Forty-eight hours after transfection, crude membranes were prepared by scraping and triturating transfected cells in standard binding buffer (SBB) (50 mM Tris-HCl, 10 mM $MgCl_2$, and 0.1 mM EDTA, pH 7.4), followed by centrifugation at 15,000 × *g* for 15 min. The membrane pellets were immediately frozen and stored at −80 °C until use. Radioligand binding assays were completed in duplicate using 96-well assay plates, and reagents were added in the following manner: 100 μl of SBB, 250 μl of vehicle (SBB) or 2× test ligands (salvinorin A or naloxone) diluted in SBB and spanning 6 orders of magnitude from 0.01 to 10,000 nM, 50 μl of 10× [^{3}H]diprenorphine (~0.2 nM final concentration), and 100 μl of cell membranes diluted in SBB. Saturation binding assays were completed as described above using eight [^{3}H]diprenorphine concentrations ranging from ~0.02 to 2 nM in the presence or absence of 10 μM naloxone to determine nonspecific binding. The binding reactions were incubated for 1.5 h at room temperature and terminated by filtration through Whatman GF/C filters. Radioactivity was determined using a Beckman Coulter LS6500 scintillation counter.

Substituted Cysteine Accessibility Method—These experiments were completed as previously described (19, 20).

KOR Modeling and Ligand Docking—Modeling studies were performed using SYBYL (version 7.1; Tripos Associates, Inc., St. Louis, MO). Initial receptor models described in this work are derived from our previously published KOR-salvinorin A interaction model (10). In order to explore the possible role of Val-2.63^{118} in our KOR model, an extracellular portion of TM2 (Met-112(2.57) to Met-121(2.66)) was rotated so as to position Val-118(2.63) to interact either with the ligand directly or with other nearby features of the KOR, particularly the E1 and E2 loops. Two separate rotations were applied to the extracellular portion of TM2 in our KOR model using a SYBYL Programming Language script developed in house. The overall rotation of this part of TM2 was performed as two separate rotations rather than one to prevent severe distortions at the TM2-E1 loop interface. For the first of the two rotations, an axis of rotation was defined by residues Ile-96(2.41) to Val-108(2.53) (Axis 1). Residues Met-112(2.57) to Met-121(2.66) were then rotated by −30.0° about Axis 1 (counterclockwise when looking at the extracellular portion of the KOR from the extracellular space), positioning these residues closer to TM1 and reorienting the Val-118(2.63) side chain toward TM3. For the second rotation, an axis of rotation was defined using residues Met-112(2.57) to Met-121(2.66) (Axis 2). Met-112(2.57) to Met-121(2.66) were then rotated by −45.0° about Axis 2, such that the side chain of Val-118(2.63) was positioned between the binding site and the TM2-TM3 interfacial region.

Upon completion of the rigid helix rotations, the side chain conformations of residues Pro-56 to Gly-73 on TM1 and Met-112(2.57) to Met-121(2.66) on TM2 were reassigned using SCWRL 3.0 (23). The model was then subjected to energy minimization using the Tripos force field incorporating Gasteiger-Hückel charges with a distance-dependent dielectric constant = 4 and a nonbonded cut-off = 8 Å to a gradient of 0.05 kcal/(mol × K). The resulting model possessed a helix irregularity in the helical backbone structure at Met-2.57^{112}-Pro-2.58^{113}, indicated by the ribbon backbone trace as rendered by the MOLCAD facility within SYBYL. The loop search facility within SYBYL was thus used to find a suitable replacement for the distorted section (Thr-109(2.54) to Thr-117(2.62), one turn above and below Pro-113(2.58)). The replacement sequence selected consisted of residues Leu-144 to Tyr-155 (including anchor regions; sequence homology to KOR sequence = 60%; root mean square fit to anchor regions = 0.12 Å) of the E chain of Protein Data Bank structure 1RP3, an all-helical RNA polymerase σ factor. SCWRL version 3 was used once again to assign side chain geometries to the newly substituted backbone, and the KOR model was energy-minimized under the same conditions as described above to generate what will subsequently be called the TM2-rotated KOR model. After minimization of the TM2-rotated KOR model, a helix irregularity once again appeared at Pro-113(2.58). A crystal structure (Protein Data Bank code 1U1I, residues Thr-1031 to Tyr-1043) was found that exhibited the same helix irregularity as the TM2-rotated KOR model (not shown), suggesting that this feature does occur.

The automated docking program GOLD (24, 25) (version 3.0.1) was used to dock salvinorin A into the receptor site of the TM2-rotated KOR model. The CONCORD routine within SYBYL was used to assign initial conformations to salvinorin A. Genetic algorithm and annealing parameters corresponding to the 3× speedup option in GOLD were used, and 30 individual genetic algorithm runs were performed. A 20.0-Å radius about the Tyr-313(7.36) side chain oxygen atom was used to define the receptor site. Cavity detection and ring corner flipping were enabled, and the GoldScore fitness function was used to rank the docked solutions.

To explore the possible interaction of the cognate residue of Val-118(2.63) in the DOR (Lys-108(2.63)) and the MOR (Asn-129(2.63)) with the E2 loop, molecular dynamics (MD) simulations were performed. Initial V118(2.63)K and V118(2.63)N KOR mutants were generated from the TM2-rotated KOR model by mutating the 2.63-position *in silico*. As in our previous work (10), the N terminus was removed, because it has been previously shown that the N-terminal region is not necessary for ligand binding to MOR (26, 27) and that the lengths and sequence homology of the KOR and rhodopsin loops bear little similarity. For each KOR mutant, an MD simulation was performed for 100 ps using the default settings of the MD routine within SYBYL, except that snapshots were taken every 25 fs rather than every 5 fs. Additionally, the energy setup was the same as that described above for energy minimization. All residues except the E2 loop (Val-195 to Asp-223), Cys-131, and either Lys-118(2.63) or Asn-118(2.63) were maintained as an aggregate.

For the models presented here, the PROTABLE facility within SYBYL was used to identify and adjust sites of unusual and sterically clashing side chain geometries. All molecular modeling was carried out on IRIX 6.5-based Silicon Graphics, Inc. workstations.

Data Analysis—Statistical comparisons were made using one-way analysis of variance followed by Dunnett's *post hoc* analysis for comparison of mutant or chimeric receptors with wild-type KOR as indicated. Heterologous competition and saturation binding

analyses as well as statistical comparisons were completed using GraphPad Prism 4.03 (GraphPad Software, Inc., San Diego, CA).

RESULTS

Identification of Domains Essential for Salvinorin A Binding to KOR Revealed by Analysis of Chimeric Opioid Receptors—Our previous studies have demonstrated that the lipid-like hallucinogen salvinorin A selectively and potently binds to the peptidergic KOR, with no significant affinity for the DOR or MOR subtypes (5). We took advantage of this selective binding profile to identify receptor domains involved in the subtype-selective binding of salvinorin A to KOR. To this end, a series of chimeric opioid receptors were constructed using an overlapping PCR strategy to combine transmembrane and loop segments of the KOR, DOR, and MOR (Fig. 1). All chimeras were expressed at moderate to high levels (0.74–64 pmol/mg protein) in HEK 293T cells and retained high affinity for the antagonist [^{3}H]diprenorphine, which was used to label these chimeras in competition binding studies (Table 1).

To elucidate the receptor regions that are important for salvinorin A selectivity, we first determined the affinity constants (K_i) of salvinorin A and naloxone at the $KOR_{(TM1-4,E2L)}$-$DOR_{(TM5-7)}$ and $DOR_{(TM1-4,E2L)}$-$KOR_{(TM5-7)}$ chimeras. The $KOR_{(TM1-4,E2L)}$-$DOR_{(TM5-7)}$ chimera exhibited an affinity for salvinorin A comparable with wild-type KOR, whereas the affinity of salvinorin A at the $DOR_{(TM1-4,E2L)}$-$KOR_{(TM5-7)}$ chimera was similar to wild-type DOR (Table 1 and Fig. 2*A*). The affinity of the nonselective antagonist naloxone for the $KOR_{(TM1-4,E2L)}$-$DOR_{(TM5-7)}$ and $DOR_{(TM1-4,E2L)}$-$KOR_{(TM5-7)}$ chimeras was comparable with wild-type KOR and DOR, respectively (Table 1 and Fig. 2*B*), suggesting that the lack of salvinorin A binding at the $DOR_{(TM1-4,E2L)}$-$KOR_{(TM5-7)}$ chimera did not result from a global disruption of the receptor ligand binding pocket.

To further identify specific receptor domains within the proximal

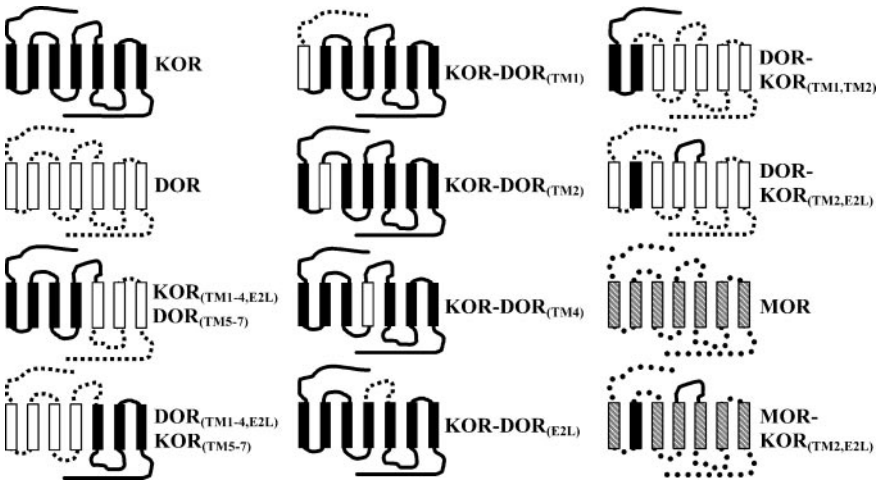

FIGURE 1. **Schematic diagrams of wild-type KOR, DOR, MOR, and selected cross-subtype chimeras.** Ten functional chimeras between KOR (*black*), DOR (*white*), and MOR (*hatched*) were constructed as described under "Experimental Procedures." The KOR-DOR chimeras included $KOR_{(TM1-4,E2L)}$-$DOR_{(TM5-7)}$ and $DOR_{(TM1-4,E2L)}$-$KOR_{(TM5-7)}$ and the single TM chimeras, including KOR-$DOR_{(TM1)}$, KOR-$DOR_{(TM2)}$, KOR-$DOR_{(TM4)}$, and KOR-$DOR_{(E2L)}$, in which the indicated receptor domains of DOR were substituted into KOR. The KOR-$DOR_{(TM2)}$ chimera also contained a similar amino acid mutation (M90L) in the first intracellular loop of KOR. The salvinorin A rescue chimeras included DOR-$KOR_{(TM1)}$ (not shown), DOR-$KOR_{(TM1,TM2)}$, DOR-$KOR_{(TM2,E2L)}$, and MOR-$KOR_{(TM2,E2L)}$, in which the indicated receptor domains of KOR were substituted into DOR or MOR as indicated. The DOR-$KOR_{(TM2,E2L)}$ chimera also contained a similar amino acid mutation (L80M) in the first intracellular loop of DOR. Two additional receptors were constructed using site-directed mutagenesis in the DOR-$KOR_{(TM2,E2L)}$ and MOR-$KOR_{(TM2,E2L)}$ chimeras to revert the nonconserved amino acids (Thr-2.55 and Met-2.57) in TM2 of KOR to the analogous residues (Ser-2.55 and Leu-2.57) in wild-type DOR and MOR. These chimeric/mutant receptors were used to assess more directly the role of Val-2.53 and Val-2.63 in rescuing salvinorin A binding to MOR and DOR.

TABLE 1
Affinity constants (K_i) for salvinorin A and naloxone binding to wild-type KOR, DOR, and MOR and cross-subtype chimeras

Receptor	K_d[a]	B_{max}[a]	Salvinorin A		Naloxone	
			K_i[b]	Ratio[c]	K_i[b]	Ratio[c]
	nM	pmol/mg	nM		nM	
KOR	0.15 ± 0.02	6.9 ± 0.3	27.1 ± 4.7		11.9 ± 1.4	
$KOR_{(TM1-4,E2L)}$-$DOR_{(TM5-7)}$	0.08 ± 0.02	3.2 ± 0.4	18.2 ± 3.0	0.7	5.2 ± 0.8	0.4
DOR	0.40 ± 0.01	4.7 ± 0.2	>10,000[d,e]	>350	54.9 ± 6.4[d]	4.6
$DOR_{(TM1-4,E2L)}$-$KOR_{(TM5-7)}$	0.94 ± 0.11	12.3 ± 0.1	>10,000[d,e]	>350	74.9 ± 9.2[d]	6.3
KOR-$DOR_{(TM1)}$	0.43 ± 0.08	48.9 ± 5.6	14.5 ± 5.8	0.5	22.5 ± 2.5	1.9
KOR-$DOR_{(TM2)}$	0.82 ± 0.16	22.9 ± 1.4	>10,000[d,e]	>350	37.4 ± 2.6[d]	3.1
KOR-$DOR_{(TM4)}$	0.16 ± 0.02	48.3 ± 10.2	95.6 ± 21.1	3.5	8.2 ± 0.6	0.7
KOR-$DOR_{(E2L)}$	0.14 ± 0.05	10.3 ± 0.8	204 ± 55[d]	7.5	9.9 ± 0.6	0.8
DOR-$KOR_{(TM1)}$	0.33 ± 0.04	13.9 ± 1.0	>5000[d,e]	>180	25.0 ± 3.5	2.1
DOR-$KOR_{(TM1,TM2)}$	0.31 ± 0.05	64.1 ± 2.9	854 ± 67[d]	31.5	13.3 ± 2.7	1.1
DOR-$KOR_{(TM2,E2L)}$	0.06 ± 0.01	0.75 ± 0.01	128 ± 21[d]	4.7	9.4 ± 1.2	0.8
DOR-$KOR_{(TM2,E2L)}$ T2.55S,M2.57L	0.062 ± 0.002	2.2 ± 0.1	54.3 ± 9.7	2.0	8.12 ± 0.01	0.7
MOR	0.17 ± 0.05	2.0 ± 0.4	>1000[d,e]	>37	4.4 ± 0.2	0.4
MOR-$KOR_{(TM2,E2L)}$	0.048 ± 0.004	0.321 ± 0.003	19.6 ± 2.1	0.7	0.6 ± 0.1	0.1
MOR-$KOR_{(TM2,E2L)}$ T2.55S,M2.57L	0.04 ± 0.01	0.74 ± 0.03	22.4 ± 2.6	0.8	0.27 ± 0.03	0.02

[a] Saturation binding of [^{3}H]diprenorphine for wild-type KOR, DOR, and MOR and cross-subtype chimeras was performed in transiently transfected HEK 293T cells. Data shown are the mean ± S.E. of two or three independent experiments performed in duplicate.
[b] The affinity constants (K_i) for salvinorin A and naloxone were determined by heterologous competition binding using [^{3}H]diprenorphine and increasing concentrations of unlabeled ligands. Data shown are the mean ± S.E. for at least three independent experiments performed in duplicate. For K_i values of >10,000 nM, inhibition was less than 50% with 10 μM salvinorin A.
[c] For each compound, the ratio is $K_{i(chimera)}/K_{i(KOR)}$.
[d] $p < 0.01$ compared with wild-type KOR for the indicated ligand (Dunnett's *post hoc* one-way analysis of variance).
[e] Inhibition less than 50%.

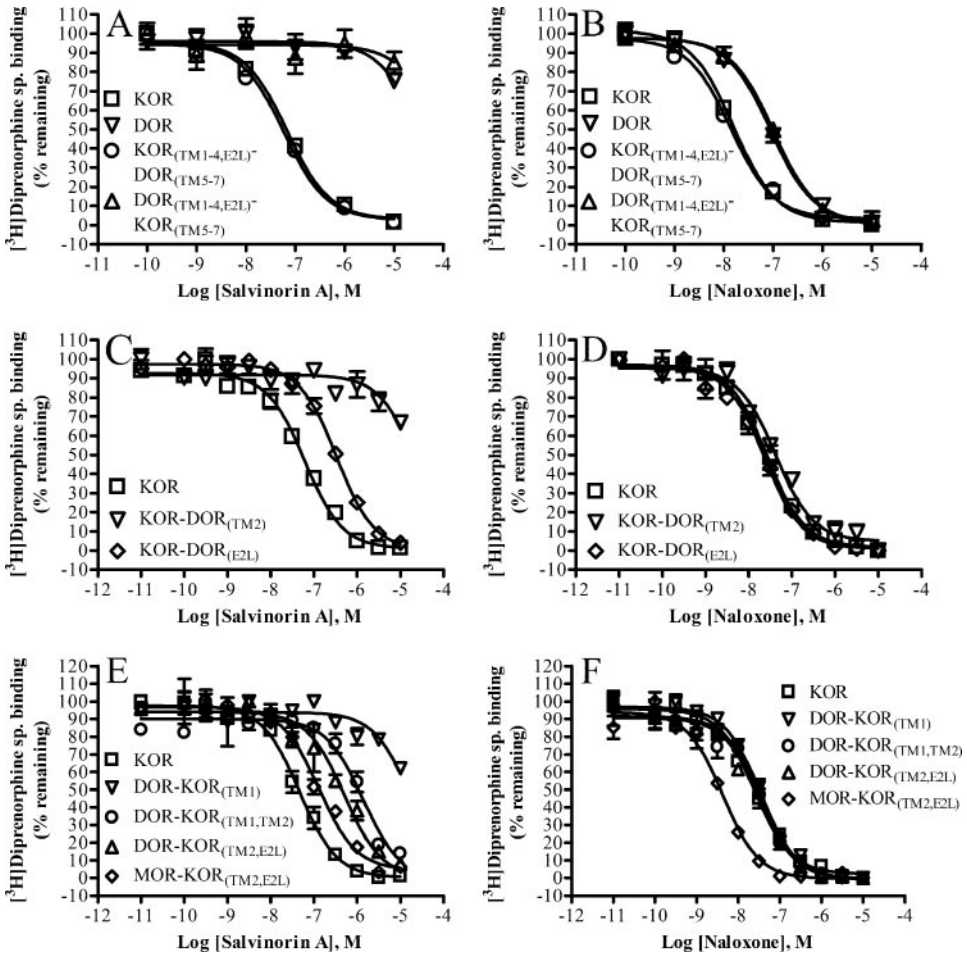

FIGURE 2. **Identification of TM2 and the E2 loop as essential domains for subtype selectivity using chimeric opioid receptors.** Representative competition binding isotherms for salvinorin A and naloxone at wild-type and various chimeric opioid receptors are shown. The data are presented as the percentage of total [^{3}H]diprenorphine binding (~0.2 nM) in the presence of increasing concentrations of unlabeled salvinorin A (*A*, *C*, and *E*) and naloxone (*B*, *D*, and *F*) as indicated. Affinity constants (see Table 1) were determined by fitting the data to a one-site competition model of radioligand binding to a single binding site using Prism 4.03 (GraphPad Software).

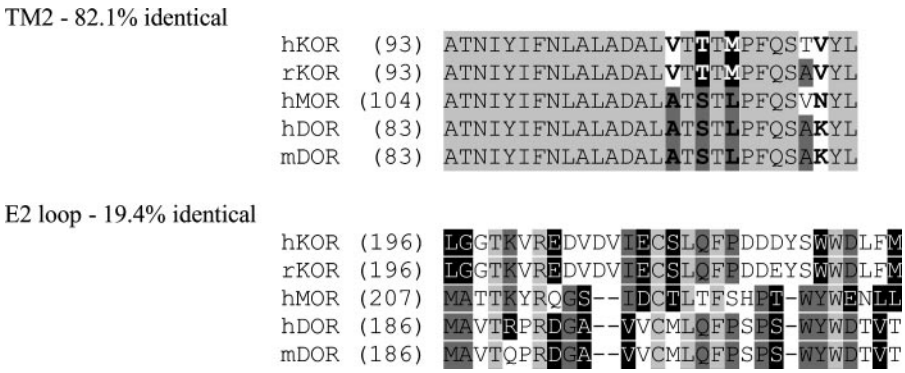

FIGURE 3. **Alignment of opioid receptor domains shown to be involved in the selectivity of salvinorin A binding.** Shown are the amino acid sequence alignments for TM2 and the E2 loop of human KOR (P41145), rat KOR (P34975), human DOR (P41143), mouse DOR (P32300), and human MOR (P35372), with the residue positions shown in *parentheses*. The conservative and identical residues are shown in *dark* and *light gray*, respectively. The similar residues are highlighted in *black*, and nonsimilar or weakly similar residues are highlighted in *white*. Residues at positions 2.53, 2.55, 2.57, and 2.63 are indicated in *boldface type*. The sequence alignments were completed with AlignX, a component of Vector NTI Advance 10.0.1 (Invitrogen).

region (TM1–TM4 and the E2 loop) of KOR, we systematically introduced TM domains from the "salvinorin A-insensitive" DOR into the "salvinorin A-sensitive" KOR (Fig. 1) and determined the effects on salvinorin A binding affinity. The affinity constants for salvinorin A at the KOR-DOR$_{(TM1)}$ and KOR-DOR$_{(TM4)}$ chimeras were not significantly altered compared with the wild-type KOR (Table 1), indicating that the substitution of TM1 or TM4 of DOR into KOR was not sufficient to disrupt salvinorin A-KOR binding interactions. In contrast, the affinity of salvinorin A at the KOR-DOR$_{(E2L)}$ chimera was decreased 8-fold compared with wild-type KOR, and salvinorin A failed to bind at the KOR-DOR$_{(TM2)}$ chimera (Table 1 and Fig. 2*C*). All of these single TM domain chimeras, including the KOR-DOR$_{(TM2)}$ chimera, retained high affinity binding for naloxone (Table 1 and Fig. 2*D*), indicating that the lack of salvinorin A binding to the KOR-DOR$_{(TM2)}$ chimera was not caused by a global disruption of the ligand binding pocket.

Since introduction of TM2 and the E2 loop of DOR markedly reduced salvinorin A binding in KOR, we performed the converse rescue experiments. In these experiments, "salvinorin A-sensitive" KOR domains were introduced into the "salvinorin A-insensitive" DOR and MOR subtypes (Fig. 1), and we determined the affinity of salvinorin A and naloxone. Two additional receptors were constructed using site-directed mutagenesis in the DOR-KOR$_{(TM2,E2L)}$ and MOR-KOR$_{(TM2,E2L)}$ chimeras to revert the nonconserved but similar amino acids (Thr-2.55 and Met-2.57) in TM2 of KOR to the analogous residues (Ser-2.55 and Leu-2.57) in wild-type DOR and MOR (Fig. 3). These receptors were used to assess more directly the role of the divergent residues (Val-2.53 and Val-2.63) in rescuing salvinorin A binding to MOR and DOR. The affinity of [^{3}H]diprenorphine for the MOR-KOR and DOR-KOR rescue chimeras was modestly increased (4- and 7-fold) compared with wild-type MOR and DOR, respectively (Table 1). The affinity of naloxone at the MOR-KOR$_{(TM2,E2L)}$ and MOR-KOR$_{(TM2,E2L)}$ T2.55S,M2.57L chimeras was increased (7- and 16-fold, respectively) compared with wild-

TABLE 2
Affinity constants (K_i) for salvinorin A and naloxone binding to wild-type and mutant KORs

Receptor	K_d [a]	B_{max} [a]	Salvinorin A		Naloxone	
			K_i [b]	Ratio [c]	K_i [b]	Ratio [c]
	nM	pmol/mg	nM		nM	
KOR	0.124 ± 0.004	7.3 ± 1.1	23.5 ± 5.7		8.5 ± 1.1	
V108(2.53)A	0.45 ± 0.06	13.2 ± 2.3	269 ± 25[d]	11.4	45.8 ± 6.9[d]	5.4
V108(2.53)L	0.11 ± 0.04	25.9 ± 11.1	4.1 ± 0.8	0.2	3.6 ± 0.6	0.4
T110(2.55)S	0.46 ± 0.12	7.8 ± 4.4	28.0 ± 5.3	1.2	15.9 ± 2.2	1.9
M112(2.57)L	0.18 ± 0.03	15.9 ± 1.2	73.5 ± 20.8	3.1	7.8 ± 0.2	0.9
V118(2.63)K	1.47 ± 0.30	21.7 ± 0.6	846 ± 176[d]	35.9	24.5 ± 2.1	2.9
V108(2.53)A,V118(2.63)K	3.20 ± 0.46	6.1 ± 2.6	>5000[d,e]	>200	107 ± 19[d]	12.5
I133(3.27)A	0.16 ± 0.03	11.2 ± 1.1	19.1 ± 4.6	0.8	12.8 ± 0.4	1.5
I135(3.29)L	0.19 ± 0.03	47.6 ± 11.2	99.1 ± 28.4	4.2	9.6 ± 0.7	1.1

[a] Saturation binding of [^{3}H]diprenorphine for wild-type and mutant KORs was performed in transiently transfected HEK 293T cells. Data shown are the mean ± S.E. of 2–4 independent experiments performed in duplicate.
[b] The affinity constants (K_i) for salvinorin A and naloxone were determined by heterologous competition binding using [^{3}H]diprenorphine and increasing concentrations of unlabeled ligands. Data shown are the mean ± S.E. of at least three independent experiments performed in duplicate.
[c] For each compound, the ratio is $K_{i(mutant)}/K_{i(KOR)}$.
[d] $p < 0.05$ compared to wild-type KOR for the indicated ligand (Dunnett's *post hoc* one-way analysis of variance).
[e] Inhibition was ~50% with 10 μM salvinorin A.

type MOR, whereas the affinity of naloxone for the DOR-KOR rescue chimeras was comparable with wild-type KOR (Table 1 and Fig. 2*F*).

As shown in Table 1 and Fig. 2*E*, the substitution of TM1 of KOR into DOR (DOR-KOR$_{(TM1)}$) had no significant effect on salvinorin A affinity compared with wild-type DOR; however, the substitution of TM1 and TM2 of KOR into DOR (DOR-KOR$_{(TM1,TM2)}$) rescued salvinorin A binding to DOR. The affinity of salvinorin A was increased further at the DOR-KOR$_{(TM2,E2L)}$ chimera in which TM2 and the E2 loop of KOR were substituted into DOR (Table 1). Similarly, the substitution of TM2 and the E2 loop of KOR into MOR (MOR-KOR$_{(TM2,E2L)}$) rescued high affinity salvinorin A binding to MOR comparable with the wild-type KOR (Table 1). Salvinorin A binding was also rescued to a comparable degree with the DOR-KOR$_{(TM2,E2L)}$ T2.55S,M2.57L and MOR-KOR$_{(TM2,E2L)}$ T2.55S,M2.57L chimeras (Table 1). These observations demonstrate a critical role for TM2 as well as the E2 loop in stabilizing salvinorin A binding interactions in DOR and MOR, but the 2.55 and 2.57 positions do not appear to be critical sites of interaction for salvinorin A.

Site-directed Mutagenesis Reveals Two Residues That Confer Salvinorin A Selectivity—All of the opioid receptors, including KOR, DOR, and MOR, share significant sequence similarities in the putative transmembrane domains (28), with >80% homology in TM2 and TM3 (Fig. 3). Sequence alignments of selected species of KOR, DOR, and MOR also revealed that TM1 and TM4 share >40% sequence identity (not shown), whereas the E2 loop regions of opioid receptors are mostly divergent (Fig. 3). Based on the observation that the KOR-DOR$_{(TM2)}$ chimera lacks the ability to bind salvinorin A and the DOR-KOR$_{(TM2,E2L)}$ and MOR-KOR$_{(TM2,E2L)}$ chimeras exhibit a significant gain in salvinorin A affinity, we focused our attention on the nonconserved amino acid residues within TM2 of KOR, including Val-108(2.53), Thr-110(2.55), Met-112(2.57), and Val-118(2.63) (Fig. 3, shown in *boldface type*). The amino acid at position 2.62 (Thr-117) of human KOR is not conserved in DOR, but the analogous residue in rat KOR (Ala-117(2.62)) is conserved with DOR Ala-107(2.62) (Fig. 3). Since salvinorin A binds to the rat KOR with high affinity, we reasoned that the sequence divergence between human KOR and DOR at position 2.62 is not likely to account for the selectivity of salvinorin A binding. The nonconserved amino acids were mutated one at a time to the analogous residues in DOR (Ala-98(2.53), Ser-100(2.55), Leu-102(2.57), and Lys-108(2.63)), and the affinity constants for salvinorin A and naloxone at wild-type and mutant KORs were determined.

As shown in Table 2 and Fig. 4, *A* and *B*, only the V108(2.53)A and V118(2.63)K mutations caused a statistically significant decrease in salvinorin A affinity. The V108(2.53)A mutation decreased salvinorin A 11-fold and naloxone affinity 5-fold, whereas the V118(2.63)K mutation markedly decreased salvinorin A affinity 36-fold but caused only a slight decrease (3-fold) in the affinity of naloxone compared with wild-type KOR (Table 2). The double mutation of V108(2.53)A and V118(2.63)K dramatically decreased salvinorin affinity >200-fold and naloxone affinity 12-fold (Table 2 and Fig. 4). The double mutant of KOR also decreased the affinity of [^{3}H]diprenorphine 20-fold compared with wild-type KOR (Table 2). We also utilized site-directed mutagenesis to examine the nonconserved residues in TM3, which were not examined in our chimeric studies. Mutation of the nonconserved amino acids in TM3 of KOR (Ile-133(3.27) and Ile-135(3.29)) to the analogous residues in DOR (Ala-123(3.27) and Leu-125(3.29)) had negligible effects on the affinity of salvinorin A and naloxone compared with wild-type KOR (Table 2). Taken together, these findings demonstrate crucial roles for Val-108(2.53) and Val-118(2.63) in mediating the subtype selectivity of salvinorin A to KOR.

Molecular Modeling Predicts Differential TM2 Helical Orientations among Opioid Receptor Subtypes—Our initial KOR model (10) was subsequently modified to incorporate and account for the experimentally determined binding data presented here. Mutant KOR models V118(2.63)K and V118(2.63)N were also created to explore indirect effects that may be occurring at the DOR and MOR receptors, respectively, thus preventing salvinorin A from binding at those receptor mutants. Since the initial model did not sufficiently explain the involvement of Val-118(2.63) in salvinorin A binding, an extracellular portion of TM2 was rotated so as to position Val-118(2.63) in a more prominent location in which it might be accessed from within the receptor binding site.

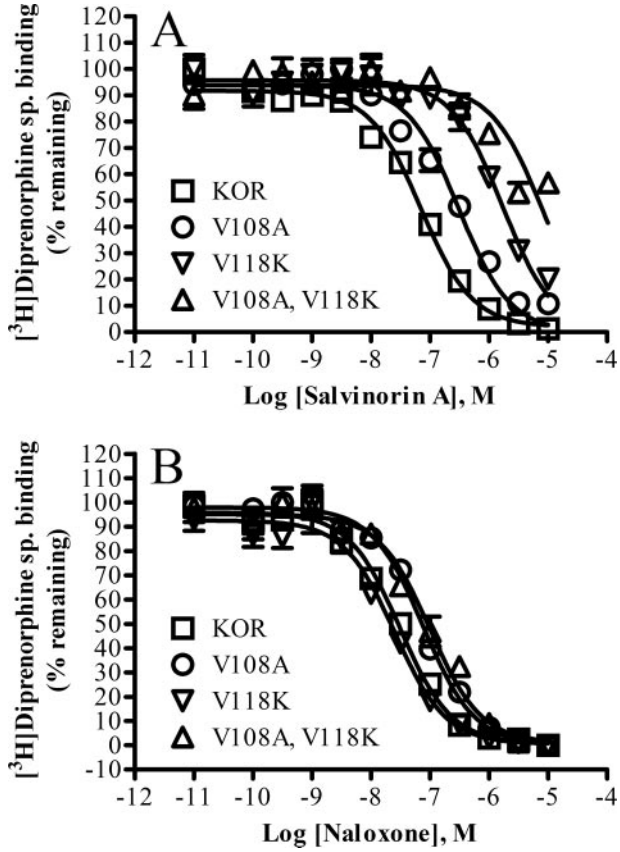

FIGURE 4. **Identification of Val-108 and Val-118 as critical residues for the subtype selectivity of salvinorin A.** Representative competition binding isotherms are shown for salvinorin A and naloxone at wild-type and mutant KORs transiently expressed in HEK 293T cells. The data are presented as the percentage of total [^{3}H]diprenorphine binding (~0.2 nM) in the presence of increasing concentrations of unlabeled salvinorin A (*A*) and naloxone (*B*) as indicated. Affinity constants (see Table 2) were determined by fitting the data to a one-site competition model of radioligand binding to a single binding site using Prism 4.03 (GraphPad Software).

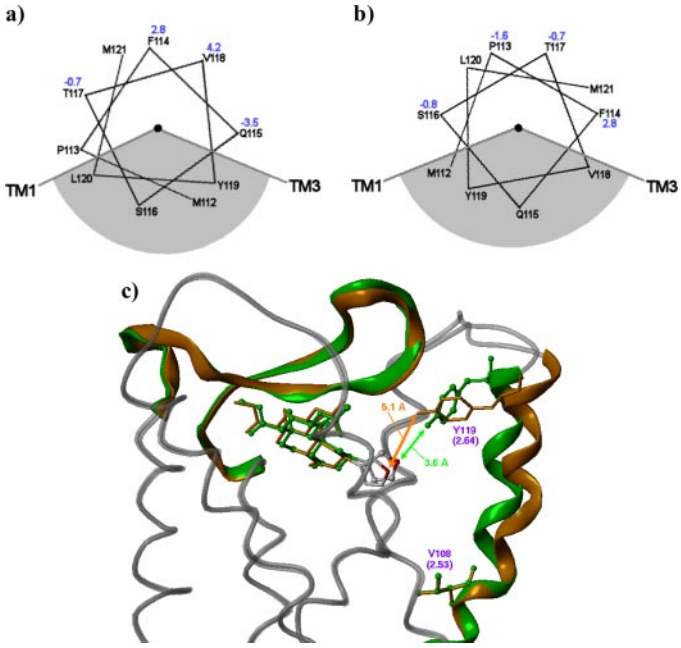

FIGURE 5. **Molecular modeling and SCAM predict a helical rotation involved in subtype selectivity of salvinorin A.** *Wheel plots* depict the orientation of the rotated residues (Met-112 to Met-121) in TM2 before the rotations (*a*) and after the rotations (*b*) in the wild-type KOR. The *gray areas* correspond to the inward facing portions of the helix; *white areas* are outward facing (toward the lipid membrane). *Numbers* in *blue* specify Kyte-Doolittle hydropathy indices. Leu-120 and Met-121 were not included. *c*, molecular models of the KOR wild-type receptor before rotation (*green*) and after rotation (*orange*) with salvinorin A docked and energy-minimized in both receptors. The differential orientation of Tyr-119(2.64) is illustrated. For clarity, the backbone trace of TM1 has been omitted.

The amount of helical rotation applied to Met-112(2.57) to Met-121(2.66) was determined visually and with the aid of wheel plots depicting the lipid- or binding site-exposed status of these residues (Fig. 5). A simple calculation involving the Kyte-Doolittle hydropathy index (29) was employed to estimate the hydrophobicity of the membrane-exposed residues before and after rotation. In Fig. 5*a*, residues Phe-114(2.59), Gln-115(2.60), Thr-117(2.62), and Val-118(2.63) are clearly lipid-exposed (Leu-120(2.65) and Met-121(2.66) were not included, since these residues were considered to be above the lipid layer at and near the polar head groups of the phospholipids). The hydropathy indices for each of the lipid-exposed residues were then summed to obtain a measure of hydrophobicity (Table 3). Small side chains that were in the interhelical space and not clearly lipid-exposed were not included in the calculation. The hydropathy score was also calculated for the lipid-exposed residues after the rotation (Fig. 5*b* and Table 3), and the two values were compared. A helix rotation was considered to be favorable if the sum of the hydropathy indices was greater after the rotation than before the rotation, since this would place side chains with more hydrophobic character into the lipid bilayer. As Table 3 indicates, helix rotations are favorable for the KOR V118(2.63)K and V118(2.63)N mutants as well as DOR and MOR but not for the wild-type KOR. These modeling results predicted that the rotational flexibility of the extracellular part of TM2 itself may be responsible for the lack of binding affinity for the KOR mutant, a prediction experimentally verified (see below).

Preliminary attempts to dock salvinorin A into the receptor binding site of the TM2-rotated KOR model using automated methods indicated that direct interaction between the salvinorin A and Val-118(2.63) is not sterically achievable. Binding modes similar to that previously proposed (10), however, were found among the docked solutions. In these docked solutions, the weak hydrogen bond interaction of Tyr-119(2.64) with the furan oxygen of salvinorin A is disrupted in the TM2-rotated KOR model (Fig. 5*c*).

Lacking a binding mode with the direct involvement of Val-118(2.63), the modeling effort was shifted toward identifying indirect effects that could give rise to the specificity of salvinorin A for KOR. MD simulations were performed with V118(2.63)K and V118(2.63)N KOR mutants. The outcome of these MD runs was quite different for each of the KOR-to-DOR (V118(2.63)K) and KOR-to-MOR (V118(2.63)N) mutants. For the V118(2.63)K mutant, the side chain of Glu-209 (E2 loop) became associated with the Lys-118(2.63) and Trp-124 (E1 loop) side chains within the first 5 ps, and this ion pair remained intact throughout the remainder of the MD trajectory. Interestingly, at the same time the ion pair was being formed, the E2 loop underwent a concerted motion that effectively reorganized the side chain interactions within the loop, modifying the

TABLE 3

The hydropathic sums calculated for the clearly lipid-exposed residues before and after rotation

The Kyte-Dolittle hydropathy index was used to estimate the hydrophobicity of membrane-exposed residues. By removing strongly hydrophilic residues from the lipid-exposed regions, rotation is favored for the KOR V118K and KOR V118N mutants, DOR, and MOR but not the wild-type KOR.

	Before rotation	After rotation	Difference	Rotate?
KOR wild type	2.8 (Phe) − 3.5 (Gln) − 0.7 (Thr) + 4.2 (Val) = 2.8	−1.6 (Pro) + 2.8 (Phe) − 0.8 (Ser) − 0.7 (Thr) = −0.3	−3.1	No
KOR V118K	2.8 (Phe) − 3.5 (Gln) − 0.7 (Thr) − 3.9 (Lys) = −5.3	−1.6 (Pro) + 2.8 (Phe) − 0.8 (Ser) − 0.7 (Thr) = −0.3	5.0	Yes
KOR V118N	2.8 (Phe) − 3.5 (Gln) − 0.7 (Thr) − 3.5 (Asn) = −4.9	−1.6 (Pro) + 2.8 (Phe) − 0.8 (Ser) − 0.7 (Thr) = −0.3	4.6	Yes
DOR wild type	2.8 (Phe) − 3.5 (Gln) + 1.8 (Ala) − 3.9 (Lys) = −2.8	−1.6 (Pro) + 2.8 (Phe) − 0.8 (Ser) +1.8 (Ala) = 2.2	5.0	Yes
MOR wild type	2.8 (Phe) − 3.5 (Gln) + 4.2 (Val) − 3.5 (Asn) = 0.0	−1.6 (Pro) + 2.8 (Phe) − 0.8 (Ser) + 4.2 (Val) = 4.6	4.6	Yes

TABLE 4

Affinity constants (K_d) and B_{max} values for [^{3}H]diprenorphine binding to cysteine substitution mutants of KOR and DOR

Saturation binding of [^{3}H]diprenorphine for wild-type KOR and DOR and cysteine mutants was performed in transiently transfected HEK 293T cells. Data shown are the mean ± S.E. of three or four independent experiments performed in duplicate and were determined by fitting the data to a saturation binding model with radioligand depletion and sharing nonspecific binding using Prism 4.03 (GraphPad Software, Inc., San Diego, CA). All KOR cysteine mutants contained the C315(7.38)S background mutation.

Receptor	K_d[a]	$K_{mut}/K_{wild\ type}$	B_{max}[a]	Receptor	K_d[a]	$K_{mut}/K_{wild\ type}$	B_{max}[a]
	nM		*fmol/mg*		*nM*		*fmol/mg*
KOR	0.11 ± 0.03		99 ± 17	DOR	0.56 ± 0.22		422 ± 50
L120(2.65)C	0.25 ± 0.04	2.2	71 ± 7	L110(2.65)C	0.40 ± 0.22	0.7	116 ± 12
Y119(2.64)C	0.25 ± 0.05	2.2	131 ± 19	Y109(2.64)C	0.54 ± 0.22	1.0	378 ± 29
V118(2.63)C	0.43 ± 0.11	3.8	140 ± 12	K108(2.63)C	0.20 ± 0.03	0.4	1443 ± 384
T117(2.62)C	0.28 ± 0.08	2.4	129 ± 26	A107(2.62)C	0.26 ± 0.11	0.5	122 ± 11
S116(2.61)C	0.26 ± 0.05	2.3	300 ± 19	S106(2.61)C	0.55 ± 0.26	1.0	332 ± 34
Q115(2.60)C	1.08 ± 0.29	9.4	135 ± 19	Q105(2.60)C	0.37 ± 0.05	0.7	26 ± 4
F114(2.59)C	0.38 ± 0.03	3.3	58 ± 6	F104(2.59)C	0.28 ± 0.09	0.5	16 ± 2
M112(2.57)C	0.40 ± 0.08	3.5	70 ± 1	L102(2.57)C	0.42 ± 0.21	0.7	304 ± 41
T111(2.56)C	0.35 ± 0.03	3.0	263 ± 42	T101(2.56)C	0.20 ± 0.07	0.4	375 ± 54
T110(2.55)C	0.53 ± 0.16	4.6	501 ± 24	S100(2.55)C	0.51 ± 0.22	0.9	636 ± 30
T109(2.54)C	0.44 ± 0.06	3.8	242 ± 55	T99(2.54)C	0.48 ± 0.27	0.8	480 ± 313
V108(2.53)C	0.48 ± 0.13	4.2	188 ± 19	A98(2.53)C	0.45 ± 0.23	0.8	481 ± 230
C315(7.38)S	0.50 ± 0.13	4.3	360 ± 66				

loop backbone conformation (not shown). The loop did not, however, rise significantly out of the binding pocket. In the reorganized loop structure, Ser-211 is repositioned such that its side chain occupies the same space that salvinorin A occupies in the previously proposed binding mode, providing a possible explanation for the lack of salvinorin A binding to DOR. In the original KOR model, salvinorin A is closely associated with residues of the E2 loop (Cys-210 to Phe-214); this is consistent with the observation that the composition of the E2 loop is important in determining the selectivity of the various opioid receptors for salvinorin A. In the altered loop structure, an extensive network of hydrogen bonds was formed among the charged and polar Asp, Glu, Lys, Arg, and Gln side chains that are part of the E2 loop (not shown). In contrast, in the MD simulation of the V118(2.63)N mutant, the loop remained in its original position throughout the 100-ps simulation. In this case, the Glu-209 and Asn-118(2.63) side chains are too far apart to interact effectively.

SCAM Reveals Differential TM2 Helical Orientations among Opioid Receptor Subtypes—To further examine the role of TM2 for salvinorin A binding and to test our prediction that TM2 is rotated, we used SCAM (19–21) to explore possible differences in the water accessibility and helical orientation of residues in TM2 of KOR and DOR. Given the apparent indirect role of Val-2.53 and Val-2.63 in the selective binding of salvinorin A to KOR, we reasoned that receptor subtype differences at these loci induce changes in the helical orientation of TM2, thus resulting in differential access of residues to the water-accessible salvinorin A binding pocket.

To this end, 13 consecutive residues in the extracellular portion of TM2 in KOR (Leu-120(2.65) to Val-108(2.53)) and DOR (Leu-110(2.65) to Ala-98(2.53)) were mutated, one at a time, to cysteine. Saturation binding studies using [^{3}H]diprenorphine demonstrated that these KOR and DOR cysteine mutants were expressed at moderate levels in HEK 293T cells, and the affinity for [^{3}H]diprenorphine was not markedly altered compared with wild-type KOR and DOR, although the KOR Q115(2.60)C mutant had a 7-fold decrease in [^{3}H]diprenorphine affinity (Table 4). Pretreatment with the water-soluble and sulfhydryl-reactive MTSEA reagent markedly inhibited [^{3}H]diprenorphine binding to 5 of the 13 cysteine-substituted KOR mutants (Tyr-119(2.64), Ser-116(2.61), Gln-115(2.60), Met-112(2.57), and Val-108(2.53)) compared with the C315(7.38)S background mutation (Fig. 6*A*) (19). Pretreatment with MTSEA also significantly inhibited [^{3}H]diprenorphine binding to 6 of 13 cysteine-substituted DOR mutants (Leu-110(2.65), Lys-108(2.63), Ala-107(2.62), Gln-105(2.60), Phe-104(2.59), and Leu-102(2.57)) compared with wild-type DOR (Fig. 6*B*). Interestingly, the inhibition of [^{3}H]diprenorphine binding was reduced for the L120(2.65)C mutant of KOR and the T99(2.54)C mutant of DOR following pretreatment with MTSEA (Fig. 6). These studies revealed a differential pattern of water-accessible residues in the extracellular portion of TM2 in KOR and DOR. These SCAM results are entirely consistent with our molecular modeling studies that predict that a differential rotation of TM2 in KOR, DOR, and MOR is involved in the subtype selectivity of salvinorin A.

DISCUSSION

The major finding of this paper is that the subtype selectivity of salvinorin A for KOR over other opioid receptors appears to be due to helical rotations of TM2, which differentially orient

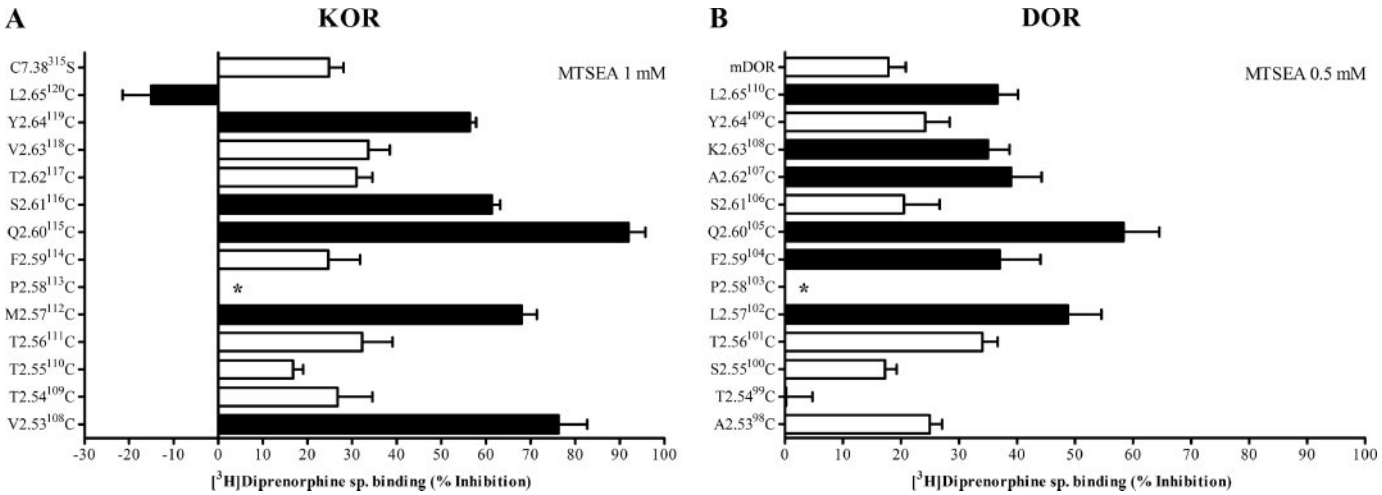

FIGURE 6. **SCAM analysis reveals a differential pattern of water accessibility in TM2 for KOR and DOR.** Cysteine-substituted mutants of the extracellular half of TM2 of KOR (*A*) and DOR (*B*) were expressed in HEK 293T cells and pretreated with the water-soluble, sulfhydryl-reactive MTSEA reagent at the indicated concentrations for 5 min. Following pretreatment, cells were washed thoroughly, and [^{3}H]diprenorphine binding (~0.2 nM) was determined using whole cell preparations. The effects of MTSEA pretreatment on [^{3}H]diprenorphine binding were expressed as percentage inhibition. Data shown are the mean ± S.E. of 3–11 independent experiments performed in duplicate. The *filled bars* indicate cysteine mutants for which MTSEA pretreatment resulted in a significant inhibition of [^{3}H]diprenorphine binding compared with the KOR C315(7.38)S mutant and wild-type DOR, respectively ($p < 0.05$, Dunnett's *post hoc* one-way analysis of variance). *, [^{3}H]diprenorphine-specific binding was too low to be accurately determined.

conserved residues for favorable interactions with salvinorin A. Classically, ligand selectivity among GPCRs has been conceived as being created by the differential interaction of selective ligands with nonconserved residues within a topologically constrained binding pocket (13, 30, 31). Our results are important, because they indicate that ligand selectivity can also be achieved by changes in the relative orientation of conserved residues within the binding pocket.

Previous studies have demonstrated that salvinorin A binding to DOR and MOR is negligible compared with KOR (5, 6), but the molecular determinants involved in this unique binding profile have yet to be determined. Our originally proposed KOR model (10) was examined in the context of the new experimental data presented here. The primary finding described in this work is that residues Val-108(2.53) and Val-118(2.63) and the E2 loop are important determinants of the selectivity of salvinorin A for the KOR. The major effect comes as a result of the KOR to DOR mutation V118(2.63)K, which shows a 36-fold decrease in the binding affinity of salvinorin A for the mutant compared with the wild type KOR. In our original model, Val-118(2.63) is oriented such that the side chain is exposed to the lipid membrane. If the mutation of Val-118(2.63) is to have a substantial effect on the binding affinity for a ligand, then it should be oriented toward the binding site or toward other structural elements of the receptor and not toward the lipid membrane. Both bovine rhodopsin and the KOR contain residues known to introduce regions of flexibility in a rigid helical structure. Bovine rhodopsin contains an underwound Gly-Gly sequence (Gly-89-Gly-90), and KOR (as well as many other aminergic GPCRs) contains a proline residue (Pro-113(2.58)) about halfway down TM2. In our initial KOR model, the underwound backbone was retained, placing Val-118(2.63) outside of the binding pocket. Performing the rotation of the extracellular portion of TM2 corresponds to taking up the slack in the underwound region and, in doing so, places Val-118(2.63) closer to the binding site and also places Tyr-119(2.64) in a different orientation. After the rotations, Val-118(2.63) was oriented between the TM2-TM3 interface and the interior binding pocket of the KOR and was flanked by Tyr-119(2.64) and Trp-124 (not shown). The SCWRL algorithm adjusted the orientation of the Tyr-119(2.64) side chain such that it remained oriented toward the interior of the binding cavity. The distance between the Tyr-119(2.64) side chain oxygen atom and the furan ring oxygen of salvinorin A increased from 3.6 to 5.1 Å after the rotation procedure and subsequent minimization, effectively preventing it from hydrogen bonding with the furan ring (Fig. 5*c*). This change is presumably a destabilizing one for salvinorin A.

As indicated under "Results," automated docking failed to find a docked solution, which showed that salvinorin A interacts with Val-118(2.63). Modeling efforts were then turned to finding possible indirect causes to explain the effect of Val-118(2.63) analogous residues on the binding of salvinorin A at DOR and MOR. These were addressed using MD and are discussed under "Results." It is tempting to suggest that the lack of binding affinity of salvinorin A for the DOR is caused by a conformational change in the structure of the E2 loop induced by the analogous residue of KOR Val-118(2.63) (DOR Lys-108(2.63)). However, if our MD simulations are correct, this conformational change would not take place in the MOR. A more likely scenario is that the rotation of the extracellular portion of TM2 itself disrupts the binding site of salvinorin A, resulting in the loss of affinity. When this rotation takes place, Tyr-119(2.64) in the KOR is reoriented such that its proposed interaction with salvinorin A is diminished relative to the unrotated helix. Additionally, if salvinorin A were to interact with other side chains on TM2 (notably Ser-116(2.61)), these would also be affected by the rotation.

Although residues on TM2 (particularly Val-108(2.53) and Val-118(2.63)) are important determinants for the selectivity of salvinorin A for KOR, the E2 loop also is important, as indicated by the DOR-KOR$_{(TM1,TM2)}$ and DOR-KOR$_{(TM2,E2L)}$ chimeras.

The substitution of TM2 of KOR into DOR rescued salvinorin A binding to a much larger degree in the presence of the KOR E2 loop (Table 1). Substitution of the E2 loop of DOR into KOR only modestly decreased salvinorin A binding (<10-fold), suggesting that the E2 loop may stabilize binding indirectly. In our original model, the hydrophobic scaffold of salvinorin A is in close proximity to Leu-212 of the E2 loop. This residue is conserved in KOR, DOR, and MOR. It is possible, however, that the differences in homology among the E2 loops of the opioid receptors confer different backbone geometries to the loops and, as a result, the position of Leu-212.

Mutagenesis and molecular modeling studies of the salvinorin A-KOR binding complex have identified multiple loci (Gln-115(2.60), Tyr-119(2.64), Tyr-313(7.36), and Tyr-320(7.43)) that are critical for stabilizing salvinorin A in the binding pocket of KOR via hydrogen bonding and hydrophobic interactions (9, 10). Our recent mutagenesis and molecular modeling studies predict that Tyr-119(2.64) and Tyr-320(7.43) stabilize salvinorin A binding via hydrogen bonds with the furan ring, and Tyr-313(7.36) is thought to form hydrophobic interactions with the methyl group of the 2-acetoxy substitution (10). Interestingly, the 2-salvinorinyl benzoate derivative preferentially interacts with the MOR subtype (32). Our binding model predicts the binding of the 2-salvinorinyl benzoate to KOR would be sterically hindered by Tyr-313(7.36), which is consistent with the loss of affinity that is observed experimentally (32). Our data imply that Val-2.53 and Val-2.63 induce changes in the orientation of Tyr-119 and/or other critical residues in the ligand binding pocket that alter the selectivity of opioid receptors for salvinorin A and derivatives.

Recently, an alternative salvinorin A-KOR binding model has been proposed by Kane *et al.* (9) in which salvinorin A is aligned vertically in the ligand binding pocket. Although this alternative model utilizes residues similar to those described herein, there are some qualitative differences in the types of binding interactions (10). In addition, the alternative model predicts that Gln-115(2.60), which appears to be water-accessible in KOR (Fig. 6), forms hydrogen bonds with the lactone oxygen(s) in the salvinorin A backbone (9). Incidentally, it is known that the 17-deoxy form of salvinorin A has high affinity (K_i = 6 nM) for the KOR (33), which would indicate that only the sp^3 oxygen is required. In addition, ligand selectivity at the KOR has been attributed to TM6; however, the data Kane *et al.* (9) indicate that Glu-297(6.58) does not appear to be involved in salvinorin A binding. Our present data do not support this alternate binding model for salvinorin A.

Intriguingly, many of the critical salvinorin A binding residues, including Gln-115(2.60), Tyr-119(2.65), and Tyr-320(7.43), are conserved in the "salvinorin A-sensitive" KOR and the "salvinorin A-insensitive" DOR and MOR subtypes. Our modeling results predict that these conserved residues exhibit differential accessibility to the salvinorin A binding pocket among the various opioid receptor subtypes. To biochemically test this prediction, we utilized SCAM to identify receptor-subtype differences in the water accessibility of residues in TM2 that line the salvinorin A binding pocket. Indeed, we identified several key differences in the water accessibility of residues in TM2 of KOR and DOR. Importantly, the conserved residue Tyr-119(2.64), which is thought to stabilize salvinorin A binding via hydrogen bonding with the furan ring of salvinorin A (10), is water-accessible in KOR but not in DOR (Fig. 6*A*). The key residues identified in the present study also exhibited a differential pattern of water accessibility. The Val-108(2.53) residue is water-accessible in KOR, whereas the analogous residue (Ala-98(2.53)) in DOR is not. This is intriguing, since Val/Ala-2.53 is positioned on the cytoplasmic side of the proline kink. Presumably, significant rotation of the cytoplasmic side of TM2 would be undesirable, since it would disrupt the interaction of Asp-2.50 with Asn-1.50 and/or Asn-7.49. Thus, Ala-98(2.53) in DOR might simply be obscured by the side chain of another nearby residue, rendering it sterically inaccessible to MTSEA. Conversely, the Lys-108(2.63) locus is water-accessible in DOR, but Val-118(2.63) of KOR is not accessible. In addition, SCAM analysis of TM7 demonstrated that the conserved residue Tyr-320(7.43), which is located in the binding site crevice of KOR and is critical for salvinorin A binding (9, 10, 21), is water-accessible in KOR but not in DOR (21).

Prior SCAM analysis of TM7 has also suggested that the nonconserved residue (Tyr-313(7.36)), which is known to interact with salvinorin A, is not water-accessible in KOR or DOR (21), although quite recent studies in our laboratory suggest that Tyr-313(7.36) has some degree of water accessibility.[3]

In summary, biochemical studies support the hypothesis that sequence divergence at the Val-2.53 and Val-2.63 loci in KOR, DOR, and MOR results in a differential pattern of residues that would have access to the salvinorin A binding pocket, thus precluding salvinorin A binding to DOR and MOR. The selectivity of salvinorin A for KOR over DOR and MOR is probably due to a rotation of the extracellular portion of TM2 when compared with the KOR. This rotation is predicted to disrupt the previously proposed salvinorin A binding site (and Tyr-119 in particular), thus accounting for the loss of affinity of salvinorin A for the DOR and MOR. These findings support a novel mode by which subtype selectivity for GPCR ligands is induced by a change in the topology of conserved residues within a common binding pocket.

Acknowledgments—We thank Ryan Strachan and Feng Yan for careful review of the manuscript and Jon Birkes and Arpan Patel for technical assistance. We also thank Dr. Thomas Prisinzano for kindly providing salvinorin A.

REFERENCES

1. Valdes, L. J., III, Diaz, J. L., and Paul, A. G. (1983) *J. Ethnopharmacol.* **7,** 287–312
2. Valdes, L. J., III (1994) *J. Psychoactive Drugs* **26,** 277–283
3. Siebert, D. J. (1994) *J. Ethnopharmacol.* **43,** 53–56
4. Sheffler, D. J., and Roth, B. L. (2003) *Trends Pharmacol. Sci.* **24,** 107–109
5. Roth, B. L., Baner, K., Westkaemper, R., Siebert, D., Rice, K. C., Steinberg, S., Ernsberger, P., and Rothman, R. B. (2002) *Proc. Natl. Acad. Sci. U. S. A.* **99,** 11934–11939
6. Chavkin, C., Sud, S., Jin, W., Stewart, J., Zjawiony, J. K., Siebert, D. J., Toth, B. A., Hufeisen, S. J., and Roth, B. L. (2004) *J. Pharmacol. Exp. Ther.* **308,** 1197–1203

[3] F. Yan and B. L. Roth, manuscript in preparation.

7. Nichols, D. E. (2004) *Pharmacol. Ther.* **101,** 131–181
8. Eguchi, M. (2004) *Med. Res. Rev.* **24,** 182–212
9. Kane, B. E., Nieto, M. J., McCurdy, C. R., and Ferguson, D. M. (2006) *FEBS J.* **273,** 1966–1974
10. Yan, F., Mosier, P. D., Westkaemper, R. B., Stewart, J., Zjawiony, J. K., Vortherms, T. A., Sheffler, D. J., and Roth, B. L. (2005) *Biochemistry* **44,** 8643–8651
11. Kristiansen, K. (2004) *Pharmacol. Ther.* **103,** 21–80
12. Ballesteros, J. A., Shi, L., and Javitch, J. A. (2001) *Mol. Pharmacol.* **60,** 1–19
13. Shapiro, D. A., Kristiansen, K., Kroeze, W. K., and Roth, B. L. (2000) *Mol. Pharmacol.* **58,** 877–886
14. Shapiro, D. A., Kristiansen, K., Weiner, D. M., Kroeze, W. K., and Roth, B. L. (2002) *J. Biol. Chem.* **277,** 11441–11449
15. Shi, L., Simpson, M. M., Ballesteros, J. A., and Javitch, J. A. (2001) *Biochemistry* **40,** 12339–12348
16. Shi, L., and Javitch, J. A. (2004) *Proc. Natl. Acad. Sci. U. S. A.* **101,** 440–445
17. Javitch, J. A., Shi, L., Simpson, M. M., Chen, J., Chiappa, V., Visiers, I., Weinstein, H., and Ballesteros, J. A. (2000) *Biochemistry* **39,** 12190–12199
18. Javitch, J. A., Ballesteros, J. A., Weinstein, H., and Chen, J. (1998) *Biochemistry* **37,** 998–1006
19. Xu, W., Chen, C., Huang, P., Li, J., de Riel, J. K., Javitch, J. A., and Liu-Chen, L. Y. (2000) *Biochemistry* **39,** 13904–13915
20. Xu, W., Li, J., Chen, C., Huang, P., Weinstein, H., Javitch, J. A., Shi, L., de Riel, J. K., and Liu-Chen, L. Y. (2001) *Biochemistry* **40,** 8018–8029
21. Xu, W., Campillo, M., Pardo, L., Kim de Riel, J., and Liu-Chen, L. Y. (2005) *Biochemistry* **44,** 16014–16025
22. Morgenstern, J. P., and Land, H. (1990) *Nucleic Acids Res.* **18,** 1068
23. Canutescu, A. A., Shelenkov, A. A., and Dunbrack, R. L., Jr. (2003) *Protein Sci.* **12,** 2001–2014
24. Jones, G., and Willett, P. (1995) *Curr. Opin. Biotechnol.* **6,** 652–656
25. Jones, G., Willett, P., Glen, R. C., Leach, A. R., and Taylor, R. (1997) *J. Mol. Biol.* **267,** 727–748
26. Watson, B., Meng, F., and Akil, H. (1996) *Neurobiol. Dis.* **3,** 87–96
27. Meng, F., Hoversten, M. T., Thompson, R. C., Taylor, L., Watson, S. J., and Akil, H. (1995) *J. Biol. Chem.* **270,** 12730–12736
28. Chen, Y., Mestek, A., Liu, J., and Yu, L. (1993) *Biochem. J.* **295,** 625–628
29. Kyte, J., and Doolittle, R. F. (1982) *J. Mol. Biol.* **157,** 105–132
30. Setola, V., Dukat, M., Glennon, R. A., and Roth, B. L. (2005) *Mol. Pharmacol.* **68,** 20–33
31. Sharma, S. K., Jones, R. M., Metzger, T. G., Ferguson, D. M., and Portoghese, P. S. (2001) *J. Med. Chem.* **44,** 2073–2079
32. Harding, W. W., Tidgewell, K., Byrd, N., Cobb, H., Dersch, C. M., Butelman, E. R., Rothman, R. B., and Prisinzano, T. E. (2005) *J. Med. Chem.* **48,** 4765–4771
33. Munro, T. A., Rizzacasa, M. A., Roth, B. L., Toth, B. A., and Yan, F. (2005) *J. Med. Chem.* **48,** 345–348